The chromodielectric soliton model: quark self-energy and hadron bags

L. Wilets,[1,*] S. Hartmann,[2,†] and P. Tang[1,‡]
[1]*Department of Physics, Box 351560, University of Washington, Seattle, Washington 98195-1560*
[2]*Sektion Physik der Universität München, Theresienstrasse 37, D-80333 München, Germany*
(Received 18 July 1996)

The chromodielectric soliton model is Lorentz and chirally invariant. It has been demonstrated to exhibit dynamical chiral symmetry breaking and spatial confinement in the locally uniform approximation. We here study the full nonlocal quark self-energy in a color-dielectric medium modeled by a two-parameter Fermi function. Here color confinement is manifest. The self-energy thus obtained is used to calculate quark wave functions in the medium which, in turn, are used to calculate the nucleon and pion masses in the one-gluon-exchange approximation. The nucleon mass is fixed to its empirical value using scaling arguments; the pion mass (for massless current quarks) turns out to be small but nonzero, depending on the model parameters. [S0556-2813(97)00804-2]

PACS number(s): 12.39.Fe, 11.30.Rd, 14.20.Dh, 14.80.Mz

I. INTRODUCTION

The chromodielectric soliton model (CDM) [1] is a Lorentz and chirally invariant low-energy effective field theory based on quantum chromodynamics (QCD). In order to simulate gluon condensates and other scalar structures (such as, e.g., $q\bar{q}$ pairs) inside hadrons the QCD Lagrangian density is supplemented by a scalar field σ that mediates the gluons through a color-dielectric function.

Following arguments first given by Friedberg and Lee [3], a suitably modeled colordielectric function $\kappa(\sigma)$ guarantees absolute color confinement [2]. The assumed potential of the scalar field is quartic and has two minima, one at zero and a second, deeper minimum at a finite value identified as the vacuum value σ_v. In the absence of quarks, the normal state of the σ field is at the vacuum value. In the presence of quarks and gluons, the σ field finds a minimum in the vicinity of zero; the quarks and gluons dig a hole in the vacuum. This is the origin of confinement in the model.

The CDM differs from the original Friedberg-Lee (FL) nontopological soliton model [3] in the essential feature that there is no direct quark-sigma coupling term. Thus the model is chirally invariant for massless quarks. Krein *et al.* [4] showed that for a locally uniform dielectric medium, chiral symmetry is dynamically broken if the strong coupling constant or the inverse of the color-dielectric function exceeds a critical value. Consequently, the quarks acquire an effective (''constituent'') mass. The Nambu-Goldstone boson corresponding to this symmetry breaking has been identified with the pion [5].

While the locally uniform model demonstrated *spatial confinement* and the emergence of the pion, it did not demonstrate *color confinement*. Furthermore, it was shown that the range of nonlocality of the quark self-energy was of the order of the typical hadronic length scale and hence large compared with the soliton surface. Therefore, it was deemed essential to investigate the nonlocal quark self-energy for a realistic and self-consistent soliton.

This is the problem we address in the present paper. We first obtain the linearized (Abelian) gluon propagator in an inhomogeneous color-dielectric medium. Because of the Abelian approximation, the calculation is analogous to a problem in electrodynamics. The Schwinger-Dyson equation for the quark propagator is solved along the imaginary energy axis in order to avoid mass poles on the real energy axis. Quark wave functions are obtained by solving the Dirac equation with the self-energy playing the role of a nonlocal scalar potential which is analytically continued to the real energy axis.

The mutual interaction between quarks and—in the case of mesons—antiquarks in hadrons is treated in the one-gluon-exchange (OGE) approximation. Corrections due to center-of-mass motion are taken into account approximately. Using scaling arguments, we fix the nucleon mass to its empirical value and calculate the pion mass as a function of phenomenological parameters. In the case of massless current quarks, the pion mass turns out to be small but nonzero. Since a vanishing pion mass is demanded by Goldstone's theorem, the calculated pion mass can be considered a test of the approximation schemes applied [6].

The paper is organized as follows. Section II introduces the basic features of the chromodielectric soliton model. After deriving the equations for the gluon propagator in an inhomogeneous medium (Sec. III), Sec. IV addresses the formulation of the appropriate Schwinger-Dyson equation for the quark self-energy. This self-energy is used in Sec. V as an effective nonlocal quark potential in order to determine quark wave functions in a bag. Section VI contains details of the numerical solution of the corresponding equations and presents results for the self energy. Section VII describes the calculation of hadronic properties in the OGE approximation and, finally, Sec. VIII sums up the main results and discusses future prospectives.

*Electronic address: Wilets@nuc2.phys.washington.edu
†Electronic address: Stephan.Hartmann@physik.uni-muenchen.de
‡Permanent address: Department of Technical Physics, Peking University, Beijing, China. Electronic address: Tang@ibm320h.phy.pku.edu.cn

II. MODEL

The CDM Lagrangian density is given by [4]

$$\mathcal{L}_{\rm CDM}=\overline{q}(i\gamma^\mu\partial_\mu+g_s\tfrac{1}{2}\lambda^a A^a_\mu\gamma^\mu-m_f)q-\kappa(\sigma)\tfrac{1}{4}F^a_{\mu\nu}F^{a\mu\nu}+\tfrac{1}{2}(\partial_\mu\sigma)^2-U(\sigma)+\mathcal{L}', \quad (1)$$

$$F^a_{\mu\nu}=\partial_\mu A^a_\nu-\partial_\nu A^a_\mu+g_s f^{abc}A^b_\mu A^c_\nu, \quad (2)$$

where the color SU(3) structure constants satisfy $[\lambda^a,\lambda^b]=2if^{abc}\lambda^c$, q are the quark fields, A^a_μ are the gluon fields, σ is the effective scalar field which determines the effective color-dielectric function $1\geq\kappa(\sigma)\geq 0$, and $\mathcal{L}'$ contains any necessary counterterms, gauge-fixing term, or ghosts. It is evident that the model is gauge invariant. m_f is the quark flavor (current) mass matrix. Throughout this paper we will set the current quark masses equal to zero, so that the model is also explicitly chirally invariant. The color-dielectric function $\kappa(\sigma)$ mediates the gluon field and is designed to guarantee color confinement. It has been shown [2] that the following assumptions must be satisfied: $\kappa(0)=1$ and $\kappa(\sigma_v)=\kappa'(\sigma_v)=\kappa'(0)=0$. These constraints are satisfied, e.g., by

$$\kappa(\sigma)=1+\theta(x)x^n[nx-(n+1)], \quad n>2, \quad (3)$$

with $x=\sigma/\sigma_v$. The vacuum value of the σ field is denoted by σ_v. We choose $n=3$ for simplicity; $\kappa(\sigma)$ is continuous at $x=0$.

Analogous to the FL model, the potential of the σ field is given by the quartic form

$$U(\sigma)=\frac{a}{2!}\sigma^2+\frac{b}{3!}\sigma^3+\frac{c}{4!}\sigma^4+B. \quad (4)$$

The ''bag constant'' B is fixed in terms of the other model constants so that $U(\sigma v)=0$. In the FL model, $U(\sigma)$ is chosen to be quartic in order to make the model renormalizable. Although our model is not renormalizable [due to the presence of $\kappa(\sigma)$], we stick to this form in order to minimize the numbers of free parameters in the model. We identify $U''(\sigma_v)\equiv m^2_{\rm GB}$ with the lowest 0^{++} glueball mass and define $U'(\sigma_v)=0$ [2].

We now discuss the divergences of the model in more detail. The model exhibits both infrared and ultraviolet divergences. The origin of the infrared divergence is the same as for the MIT bag model. For a spherical bag, for example, the electric monopole term of the quark self-energy diverges as $r\to\infty$. This happens in the CDM, if the color-dielectric constant vanishes as $r\to\infty$. The infrared divergence is thus associated with color confinement. However, for a color-singlet bag, no infrared divergence occurs since the self-interaction and mutual interaction terms cancel when ladder diagrams for the mutual interaction are properly calculated. The monopole term of the self-energy is ignored in the MIT bag model. Since this term is the source of color confinement in our model, we cannot neglect it.

The ultraviolet divergence is associated with the point nature of quarks. It is shown in Ref. [4] that the effective quark mass, which is generated because of dynamical chiral symmetry breaking, goes to infinity if the color-dielectric function approaches zero. This divergence is thus connected with spatial confinement. We handle this divergence by introducing an energy cutoff (asymptotic freedom). For numerical reasons, we regulate the infrared divergence by adjusting $\kappa_v=\kappa(\sigma_v)$ to a small nonzero value and discuss the limit $\kappa_v\to 0$.

III. GLUON PROPAGATOR

We assume that parts of the non-Abelian effects are effectively included in the σ field. This allows us to approximate the gluon field by its Abelian part. Hence the gluon field equations are formally identical to Maxwell's equations in an inhomogeneous medium characterized by a time-independent color-dielectric function $\kappa(\mathbf{r})$. The field equations for the vector potential $A_\mu(\mathbf{r},t)$ read (we follow here Refs. [7] and [8])

$$\partial^\mu\kappa(\mathbf{r})[\partial_\mu A_\nu-\partial_\nu A_\mu]=J_\nu(\mathbf{r},t). \quad (5)$$

Since the Abelian approximation destroys gauge invariance, the choice of gauge is part of the approximations. We choose the Coulomb gauge defined by

$$\boldsymbol{\nabla}\cdot(\kappa\mathbf{A})=0. \quad (6)$$

The $\nu=0$ component of Eq. (5) yields

$$-\boldsymbol{\nabla}\kappa(\mathbf{r})\cdot\boldsymbol{\nabla}A_0(\mathbf{r},t)=J_0(\mathbf{r},t). \quad (7)$$

The time-time component of the Green's function, D^{00}, defined by

$$A_0(\mathbf{r},t)=\int d^3r' D^{00}(\mathbf{r},\mathbf{r}')J_0(\mathbf{r}',t), \quad (8)$$

satisfies the equation

$$-\boldsymbol{\nabla}\kappa(\mathbf{r})\cdot\boldsymbol{\nabla}D^{00}(\mathbf{r},\mathbf{r}')=\delta^3(\mathbf{r}-\mathbf{r}'). \quad (9)$$

Note that $D^{00}(\mathbf{r},\mathbf{r}')$ is instantaneous.

Now consider the $\nu=i$ components of Eq. (5):

$$\kappa\partial_t^2\mathbf{A}-\nabla^2(\kappa\mathbf{A})+\boldsymbol{\nabla}\times(\kappa\mathbf{A}\times\boldsymbol{\nabla}\ \ln\kappa)=\mathbf{J}-\kappa\boldsymbol{\nabla}\partial_t A_0\equiv\mathbf{J}_{\rm tr}. \quad (10)$$

The transverse current defined by Eq. (10) can be expressed in terms of $\mathbf{J}$ using the time-time Green's function:

$$\mathbf{J}_{\rm tr}(\mathbf{r},t)=\mathbf{J}(\mathbf{r},t)-\kappa(\mathbf{r})\boldsymbol{\nabla}\int d^3r' D^{00}(\mathbf{r},\mathbf{r}')\partial_t J_0(\mathbf{r}',t). \quad (11)$$

Using current conservation $\partial_t J_0+\boldsymbol{\nabla}\cdot\mathbf{J}=0$ and performing a partial integration, we obtain

$$\mathbf{J}_{\rm tr}(\mathbf{r},t)=\mathbf{J}(\mathbf{r},t)-\kappa(\mathbf{r})\boldsymbol{\nabla}\int d^3r'[\boldsymbol{\nabla}' D^{00}(\mathbf{r},\mathbf{r}')]\cdot\mathbf{J}(\mathbf{r}',t). \quad (12)$$

We now Fourier transform the time dependence of $\mathbf{J}(\mathbf{r},t)$ and $\mathbf{A}(\mathbf{r},t)$ to $\mathbf{J}(\mathbf{r},\omega)$ and $\mathbf{A}(\mathbf{r},\omega)$. The Green's function corresponding to Eq. (10) satisfies

$$-[\nabla^2+\omega^2+\boldsymbol{\nabla}\times(\boldsymbol{\nabla}\ \ln\kappa)]\times\kappa\overleftrightarrow{D}(\mathbf{r},\mathbf{r}')=\overleftrightarrow{\delta}_{\rm tr}(\mathbf{r},\mathbf{r}'), \quad (13)$$

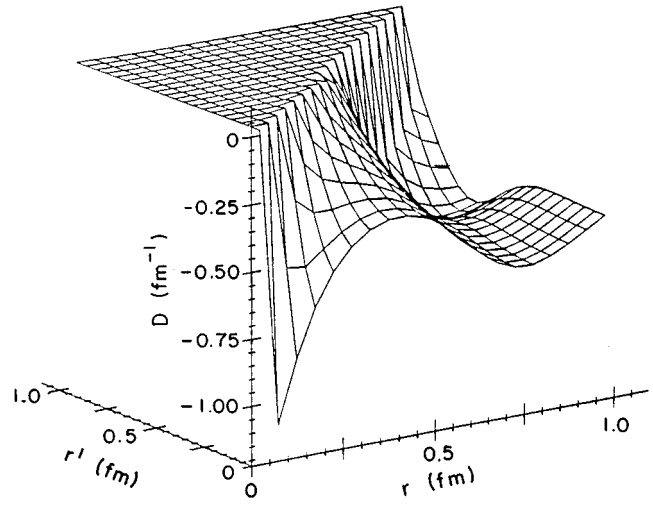

FIG. 1. The tensor part of the gluon propagator in the transverse magnetic mode $d_{102}(r,r')$.

where the components of the transverse delta function are given by

$$\delta^{ij}_{\rm tr}(\mathbf{r},\mathbf{r}')=\delta^{ij}\delta^3(\mathbf{r}-\mathbf{r}')-\kappa(\mathbf{r})\partial^i\partial'^j D^{00}(\mathbf{r},\mathbf{r}'). \quad (14)$$

In this paper we will restrict ourselves to spherical bags. In this case the Green's functions can be decomposed in terms of spherical harmonics [7]:

$$D^i_{i'}\rightarrow\overleftrightarrow{D}(\mathbf{r},\mathbf{r}';\omega)=\sum_{jll'm_l} d_{jll'}(r,r';\omega)\overleftarrow{Y}_{jlm_l}(\Omega)\vec{Y}'_{jl'm_l}(\Omega'), \quad (15)$$

$$D^{00}(\mathbf{r},\mathbf{r}')=\sum_{lm_l} d^0_l(r,r')Y_{lm_l}(\Omega)Y^*_{lm_l}(\Omega'). \quad (16)$$

Some of the tensor components are shown in Figs. 1 and 2. The $\kappa(r)$ parameters are again $R=0.8$ fm, $A=0.1$ fm, and $\kappa_v=0.1$.

It should be noted that the Green's functions do not carry any color indices. This results from the fact that the medium is color neutral so that $D_{\mu\nu}$ has a trivial (diagonal) color structure.

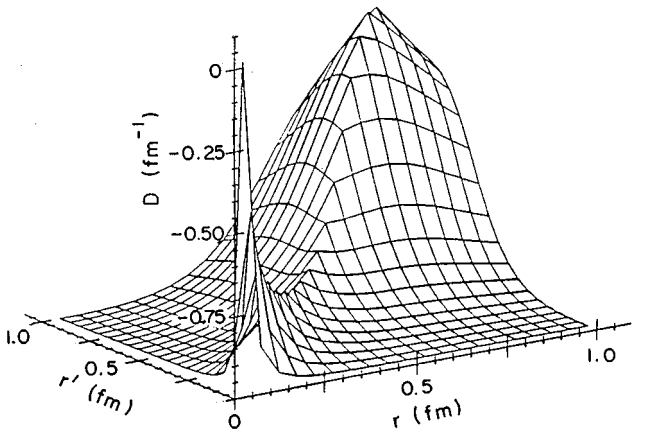

FIG. 2. The tensor part of the gluon propagator in the transverse magnetic mode $d_{122}(r,r')$.

Details of the derivation and solution of Eqs. (9) and (13) are given in [7], and an important correction is reported in Ref. [8].

IV. SCHWINGER-DYSON EQUATION IN THE QUARK-GLUON SECTOR

Being now in the possession of the gluon propagator in the cavity we can study the Schwinger-Dyson equation for a single quark in a cavity. In the course of this calculation we need not refer to the σ field.

The Schwinger-Dyson equation reads [in $(\omega,\mathbf{r})$ space]

$$\Sigma(\mathbf{r},\mathbf{r}';\omega)=i\alpha'\int_{-\infty}^{\infty}d\omega' D_{\mu\nu}(\mathbf{r},\mathbf{r}';\omega'\times\gamma^\mu S(\mathbf{r},\mathbf{r}';\omega-\omega')\gamma^\nu, \quad (17)$$

with $\alpha'=(4/3)g_s^2/2\pi$. In Eq. (17) we have already approximated the one-particle irreducible quark-gluon vertex Γ^μ by the bare one.

It is easy to show that both the gluon propagator $D_{\mu\nu}$ and the quark propagators G do not have poles off the real ω axis. So according to the Schwinger-Dyson equation, the self-energy Σ should have no pole of the real ω axis as well. Thus we perform a Wick rotation $\omega\rightarrow iy$ and study the self-energy first for imaginary ω. The ''rotated'' Schwinger-Dyson equation now reads

$$\Sigma(\mathbf{r},\mathbf{r}';y)=-\alpha'\int_{-\infty}^{\infty}dy' D_{\mu\nu}(\mathbf{r},\mathbf{r}';y')\times\gamma^\mu S(\mathbf{r},\mathbf{r}';y-y')\gamma^\nu. \quad (18)$$

Simultaneously, the Dirac equation for the quark propagator has to be satisfied:

$$(\omega\gamma^0-\boldsymbol{\gamma}\cdot\mathbf{p}-\Sigma)S=\delta^3(\mathbf{r}-\mathbf{r}'). \quad (19)$$

To simplify the notation we have used the shorthand ΣS for $\int d^3r_2\Sigma(\mathbf{r},\mathbf{r}_2;\omega)S(\mathbf{r}_2,\mathbf{r}';\omega)$. Throughout this paper repeated spatial coordinates are integrated over.

We now define the Hermitian functions

$$G=-S\beta, \quad V=\beta\Sigma. \quad (20)$$

Equations (19) and (17) then become

$$(-\omega+\boldsymbol{\alpha}\cdot\mathbf{p}+V)G=\delta^3(\mathbf{r}-\mathbf{r}'), \quad (21)$$

$$V(\mathbf{r},\mathbf{r}';y)=\alpha'\int_{-\infty}^{\infty}dy' D_{\mu\nu}(\mathbf{r},\mathbf{r}';y')\alpha^\mu G(\mathbf{r},\mathbf{r}';y-y')\alpha^\nu. \quad (22)$$

Here $\alpha^\mu\equiv(1,\boldsymbol{\alpha})$ is used for notational convenience only. It is obviously not a Lorentz vector.

From the coupled equations (21) and (22), the Hermiticity of G and V can be verified:

$$G^{\dagger}(\mathbf{r},\mathbf{r}';\omega)=G(\mathbf{r},\mathbf{r}';\omega^{*}), \tag{23}$$

$$V^{\dagger}(\mathbf{r},\mathbf{r}';\omega)=V(\mathbf{r},\mathbf{r}';\omega^{*}). \tag{24}$$

The Hermitian conjugation includes the interchange of the arguments $\mathbf{r}$ and $\mathbf{r}'$:

$$V_{ij}^{\dagger}(\mathbf{r},\mathbf{r}';\omega)\equiv V_{ji}(\mathbf{r}',\mathbf{r};\omega)^{*}. \tag{25}$$

A. Angular decomposition of the quark propagator

In order to solve the coupled equations (21) and (22) numerically, we make an angular decomposition of the appropriate quantities. For spherically symmetric color-dielectric functions $\kappa(r)$, the Hermitian properties G and V can be decomposed [9,10]:

$$G(\mathbf{r},\mathbf{r}';\omega)$$

$$=\sum_{\kappa}\begin{pmatrix} g_{\kappa}^{11}(r,r';\omega)\pi_{\kappa} & g_{\kappa}^{12}(r,r';\omega)i\sigma_{r}\pi_{-\kappa} \\ -g_{\kappa}^{21}(r,r';\omega)i\sigma_{r}\pi_{\kappa} & g_{\kappa}^{22}(r,r';\omega)\pi_{-\kappa}\end{pmatrix}, \tag{26}$$

$$V(\mathbf{r},\mathbf{r}';\omega)$$

$$=\sum_{\kappa}\begin{pmatrix} v_{\kappa}^{11}(r,r';\omega)\pi_{\kappa} & v_{\kappa}^{12}(r,r';\omega)i\sigma_{r}\pi_{-\kappa} \\ -v_{\kappa}^{21}(r,r';\omega)i\sigma_{r}\pi_{\kappa} & v_{\kappa}^{22}(r,r';\omega)\pi_{-\kappa}\end{pmatrix}, \tag{27}$$

where the respective angular part is given by the 2×2 matrices:

$$\pi_{\kappa}(\Omega,\Omega')\equiv\sum_{\mu}\mathcal{Y}_{\kappa\mu}(\Omega)\mathcal{Y}_{\kappa\mu}^{\dagger}(\Omega'). \tag{28}$$

The following reduction relationship holds:

$$\int d\Omega_{2}\pi_{\kappa}(\Omega_{1},\Omega_{2})\pi_{\kappa'}(\Omega_{2},\Omega_{3})=\delta_{\kappa\kappa'}\pi_{\kappa}(\Omega_{1},\Omega_{3}). \tag{29}$$

$\mathcal{Y}_{\kappa\mu}(\Omega)$ are the usual two-component spinor spherical harmonics. They are eigenstates of the operators J^{2}, L^{2}, J_{z}, and $K=(J+1/2)(-1)^{(J-L+1/2)}$ [2],

$$\mathcal{Y}_{\kappa\mu}(\Omega)=\sum_{m_{l},m_{s}}\langle l_{\kappa}m_{l},\tfrac{1}{2}m_{s}|j_{\kappa}\mu\rangle Y_{l_{\kappa}m_{l}}(\Omega)\chi_{m_{s}}, \tag{30}$$

and obey the orthonormality relation

$$\int d\Omega\mathcal{Y}_{\kappa\mu}^{\dagger}(\Omega)\mathcal{Y}_{\kappa'\mu'}(\Omega)=\delta_{\kappa\kappa'}\delta_{\mu\mu'}. \tag{31}$$

The radial functions g and v have the symmetry properties

$$g_{\kappa}^{ij}(r,r';\omega)=g_{\kappa}^{ji}(r',r;\omega)=g_{\kappa}^{ij}(r,r';\omega^{*})^{*}. \tag{32}$$

Inserting Eqs. (26) and (27) in the Dirac equation (21) for the quark propagator and using Eqs. (31) and (29) yields

$$\left[\begin{pmatrix} -\omega & -1/r-\partial/\partial r+\kappa/r \\ 1/r+\partial/\partial r+\kappa/r & -\omega\end{pmatrix}+\begin{pmatrix} v_{\kappa}^{11} & v_{\kappa}^{12} \\ v_{\kappa}^{21} & v_{\kappa}^{22}\end{pmatrix}\right]\times\begin{pmatrix} g_{\kappa}^{11} & g_{\kappa}^{12} \\ g_{\kappa}^{21} & g_{\kappa}^{22}\end{pmatrix}=\frac{\delta(r-r')}{rr'}, \tag{33}$$

where vg denotes $\int r_{2}^{2}dr_{2}v(r,r_{2};\omega)g(r_{2},r';\omega)$ for notational convenience.

Defining $\overline{g}(r,r';\omega)=rr'g(r,r';\omega)$ and $\overline{v}(r,r';\omega)=rr'v(r,r';\omega)$, Eq. (33) simplifies finally to

$$\left[\begin{pmatrix} -\omega & -\partial/\partial r+\kappa/r \\ \partial/\partial r+\kappa/r & -\omega\end{pmatrix}+\begin{pmatrix} \overline{v_{\kappa}^{11}} & \overline{v_{\kappa}^{12}} \\ \overline{v_{\kappa}^{21}} & \overline{v_{\kappa}^{22}}\end{pmatrix}\right]\begin{pmatrix} \overline{g_{\kappa}^{11}} & \overline{g_{\kappa}^{12}} \\ \overline{g_{\kappa}^{21}} & \overline{g_{\kappa}^{22}}\end{pmatrix}=\delta(r-r'). \tag{34}$$

Details of the nontrivial numerical solutions of this equation are discussed in Sec. VI.

B. Radial part of the Schwinger-Dyson equation

Inserting Eqs. (26) and (27) into Eq. (22), we can write

$$V(\mathbf{r},\mathbf{r}';y)=\begin{pmatrix} v_{\kappa}^{11}(r,r';\omega)\pi_{\kappa} & v_{\kappa}^{12}(r,r';\omega)i\sigma_{r}\pi_{-\kappa} \\ -v_{\kappa}^{21}(r,r';\omega)i\sigma_{r}\pi_{\kappa} & v_{\kappa}^{22}(r,r';\omega)\pi_{-\kappa}\end{pmatrix} \tag{35}$$

$$=\alpha'\int dy'D_{\mu\nu}(\mathbf{r},\mathbf{r}';y')\alpha^{\mu}G(\mathbf{r},\mathbf{r}';y-y')\alpha^{\nu}$$

$$=-\alpha'\int dy'd_{jll'}(r,r';y')\boldsymbol{\sigma}\cdot\boldsymbol{\mathcal{Y}}_{jlm}\begin{pmatrix} g_{\kappa}^{22}(r,r';\omega)\pi_{-\kappa} & -g_{\kappa}^{21}(r,r';\omega)i\sigma_{r}\pi_{\kappa} \\ g_{\kappa}^{12}(r,r';\omega)i\sigma_{r}\pi_{-\kappa} & g_{\kappa}^{11}(r,r';\omega)\pi_{\kappa}\end{pmatrix}\boldsymbol{\mathcal{Y}}_{jl'm}^{*}\cdot\boldsymbol{\sigma}$$

$$+\alpha'\int dy'd_{l}^{0}(r,r';y')Y_{lm}\begin{pmatrix} g_{\kappa}^{11}(r,r';\omega)\pi_{\kappa} & g_{\kappa}^{12}(r,r';\omega)i\sigma_{r}\pi_{-\kappa} \\ -g_{\kappa}^{21}(r,r';\omega)i\sigma_{r}\pi_{\kappa} & g_{\kappa}^{22}(r,r';\omega)\pi_{-\kappa}\end{pmatrix}Y_{lm}^{*}. \tag{36}$$

From the Appendix we find

$$\sum_m \boldsymbol{\sigma}\cdot\boldsymbol{\mathcal{Y}}_{jlm}(\Omega)\pi_\kappa(\Omega,\Omega')\boldsymbol{\sigma}\cdot\boldsymbol{\mathcal{Y}}^*_{jl'm}(\Omega') = \sum_{\kappa'} \mathcal{A}^{\kappa'\kappa}_{jll'}\pi_{\kappa'}(\Omega,\Omega'), \tag{37}$$

$$\sum_m \boldsymbol{\sigma}\cdot\boldsymbol{\mathcal{Y}}_{jlm}(\Omega)\sigma_r\pi_\kappa(\Omega,\Omega')\boldsymbol{\sigma}\cdot\boldsymbol{\mathcal{Y}}^*_{jl'm}(\Omega') = \sum_{\kappa'} \mathcal{B}^{\kappa'\kappa}_{jll'}\sigma_r\pi_{\kappa'}(\Omega,\Omega'), \tag{38}$$

$$\sum_m Y_{lm}(\Omega)\pi_\kappa(\Omega,\Omega')Y^*_{l'm}(\Omega') = \sum_{\kappa'} \mathcal{C}^{\kappa'\kappa}_l\pi_{\kappa'}(\Omega,\Omega'). \tag{39}$$

The self-energy coefficients $\mathcal{A}$, $\mathcal{B}$, and $\mathcal{C}$ are explicitly defined in the Appendix.

With these formulas the radial Schwinger-Dyson equation (36) reads

$$\overline{v}^{11}_\kappa(r,r';y) = \alpha'\int dy'[d^0_l(r,r')\overline{g}^{11}_{\kappa'}(r,r';y')\mathcal{C}^{\kappa\kappa'}_l - d_{jll'}(r,r';y')\overline{g}^{22}_{\kappa'}(r,r';y-y')\mathcal{A}^{\kappa-\kappa'}_{jll'}], \tag{40}$$

$$\overline{v}^{12}_\kappa(r,r';y) = \alpha'\int dy'[d^0_l(r,r')\overline{g}^{12}_{\kappa'}(r,r';y')\mathcal{C}^{-\kappa-\kappa'}_l + d_{jll'}(r,r';y')\overline{g}^{21}_{\kappa'}(r,r';y-y')\mathcal{B}^{-\kappa\kappa'}_{jll'}], \tag{41}$$

$$\overline{v}^{21}_\kappa(r,r';y) = \alpha'\int dy'[d^0_l(r,r')\overline{g}^{21}_{\kappa'}(r,r';y')\mathcal{C}^{\kappa\kappa'}_l + d_{jll'}(r,r';y')\overline{g}^{12}_{\kappa'}(r,r';y-y')\mathcal{B}^{\kappa-\kappa'}_{jll'}], \tag{42}$$

$$\overline{v}^{22}_\kappa(r,r';y) = \alpha'\int dy'[d^0_l(r,r')\overline{g}^{22}_{\kappa'}(r,r';y')\mathcal{C}^{-\kappa-\kappa'}_l - d_{jll'}(r,r';y')\overline{g}^{11}_{\kappa'}(r,r';y-y')\mathcal{A}^{-\kappa\kappa'}_{jll'}]. \tag{43}$$

Here we have also used Eqs. (15) and (16) as well as the symmetry properties $d^0_l(r,r')=d^0_l(r',r)$ and $d_{jll'}(r,r';\omega)=d_{jl'l}(r',r;\omega)$ which hold for both pure real and imaginary ω because in Eq. (13) for the gluon propagator only ω^2 (and not ω) appears.

V. QUARK WAVE FUNCTION

By interpreting the nonlocal self-energy as an effective potential we can now determine the wave function $q(\mathbf{r})$ and energy eigenvalue ϵ of a single quark in the cavity. The corresponding Dirac equation reads

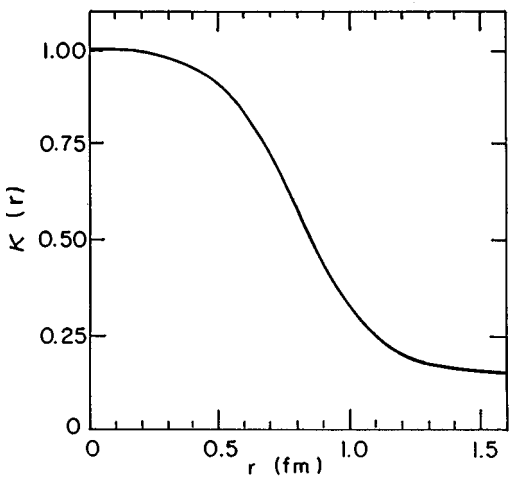

FIG. 3. The color-dielectric function $\kappa(r)$ for $R=0.8$ fm, $A=0.15$ fm, and $\kappa_v=0.15$ (r in fm).

$$\boldsymbol{\alpha}\cdot\mathbf{p}q(\mathbf{r}) + \int d^3r_2 V(\mathbf{r},\mathbf{r}_2;\epsilon)q(\mathbf{r}_2) = \epsilon q(\mathbf{r}). \tag{44}$$

In spherical coordinates, $q(\mathbf{r})$ can be written in the form [2]

$$q(\mathbf{r}) = \sum_{\kappa\mu}\begin{pmatrix} u_\kappa(r)/r \\ -i\sigma_r v_\kappa(r)/r\end{pmatrix}\otimes\mathcal{Y}_{\kappa\mu}(\Omega). \tag{45}$$

After angular decomposition, the radial part of Eq. (44) obeys

$$\begin{pmatrix} 0 & -\partial/\partial r+\kappa/r \\ \partial/\partial r+\kappa/r & 0\end{pmatrix}\begin{pmatrix} u_\kappa(r) \\ v_\kappa(r)\end{pmatrix} + \int dr_2\overline{V_\kappa}(r,r_2;\epsilon)\times\begin{pmatrix} u_\kappa(r_2) \\ v_\kappa(r_2)\end{pmatrix} = \epsilon\begin{pmatrix} u_\kappa(r) \\ v_\kappa(r)\end{pmatrix}. \tag{46}$$

VI. NUMERICAL CALCULATION

In our calculations we use a (modified) Fermi-function-shaped spherically symmetric color-dielectric function

$$\kappa(r) = \frac{1-\kappa_v}{1+e^{(r-R)/A}} + \kappa_v, \tag{47}$$

where R and A are the radius and the surface thickness, respectively, of the profile (see Fig. 3). The small but nonzero vacuum value κ_v guarantees that, e.g., the energy of a single quark in the cavity remains finite. For color-singlet multiquark systems the limit $\kappa_v\to 0$ can be performed as will be shown in Sec. VII.

Since our model is not renormalizable, an ultraviolet momentum cutoff is needed; this is consistent with asymptotic freedom. This cutoff should reflect the energy scale of the described physics; we choose $\Lambda_{\rm CDM}=5.0$ fm^{-1}. In terms of the variables used in this paper the ω' integration in Eq. (17) is cutoff at $|\omega_{\max}|=\Lambda_{\rm CDM}$ and the necessary summations over angular momenta are limited by $l_{\max}=R\omega_{\max}$ with R from Eq. (47). This procedure is not covariant, but a bag model is not covariant until projection anyway. A careful analysis of

the renormalization problem for a nonlocal, spatially varying dielectric medium can be found in Ref. [11].

With the gluon propagator derived in Sec. III, we solve the coupled equations (34) and (40)–(43) to obtain the full quark propagator and the quark self-energy on the imaginary ω axis. Because of the absence of poles in this region, the self-energy is numerically stable and no oscillations occur. A Taylor-expansion method is subsequently applied to construct the quark self-energy on the real ω axis:

$$v_\kappa(r,r';z)=v_\kappa(r,r';0)+zv'_\kappa(r,r';0)+\frac{z^2}{2}v''_\kappa(r,r';0)+\frac{z^3}{6}v^{(3)}_\kappa(r,r';0)+\frac{z^4}{24}v^{(4)}_\kappa(r,r';0)+\cdots, \tag{48}$$

where the derivatives are evaluated in terms of the discrete values of the functions along the imaginary ω axis.

Equation (34) is a coupled system of integro-differential equations. For its numerical solution we use matrix inversion. It is well known that the leap frog instability [12] (p. 342) appears in an equation like Eq. (34) when the first order derivative is replaced by a centered difference. Therefore we introduce a small second order derivative term to suppress the instability:

$$\left[\begin{pmatrix} -\omega & -\partial/\partial r+B\partial^2/\partial r^2+\kappa/r \\ \partial/\partial r+B\partial^2/\partial r^2+\kappa/r & -\omega \end{pmatrix}+\begin{pmatrix} \overline{v^{11}_\kappa} & \overline{v^{12}_\kappa} \\ \overline{v^{21}_\kappa} & \overline{v^{22}_\kappa} \end{pmatrix}\right]\begin{pmatrix} \overline{g^{11}_{B\kappa}} & \overline{g^{12}_{B\kappa}} \\ \overline{g^{21}_{B\kappa}} & \overline{g^{22}_{B\kappa}} \end{pmatrix}=\delta(r-r'), \tag{49}$$

where $B=b\Delta$ is a small number. Δ is the grid interval and $b\sim\pm1$ for $\kappa=\mp1$ (the sign is important to suppress the leapfrog effect). This additional regularizing term does not spoil the accuracy of the solution.

Numerically we find that $g_\kappa=g_{B\kappa}$ satisfies Eq. (34) very well if $B\sim\pm\Delta$. Therefore $g_{B\kappa}$ can be considered as a first approximation to g_κ. There must be a discontinuity in the Green's function for first order differential equations. In Eq. (34), this discontinuity occurs in its off-diagonal elements [10]. We find numerically that the additional second derivative term smooths out the discontinuity somewhat.

This approximation can be improved. This will be demonstrated first in general terms. Consider the following two Green's equations:

$$L_0G_0=\delta, \tag{50}$$

$$(L_0+L_B)G=\delta. \tag{51}$$

After operating with G_0 on both sides of Eq. (51) and integrating, we have

$$G_0=G_0(L_0+L_B)G=G+G_0L_BG \tag{52}$$

or

$$G=G_0-G_0L_BG. \tag{53}$$

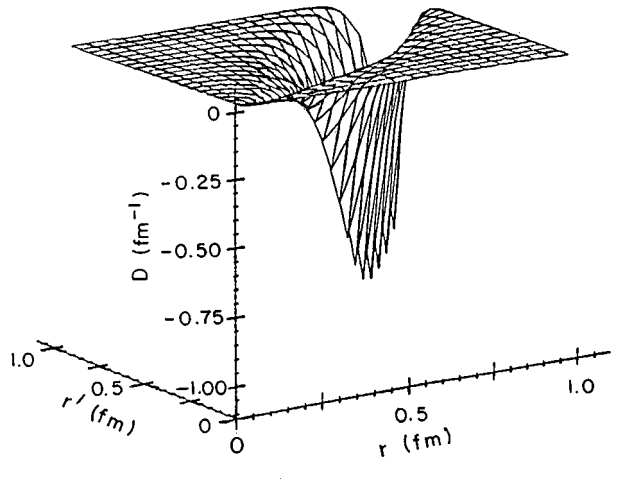

FIG. 4. The quark self-energy on the real ω axis: $\overline{v^{11}_{-1}}(r,r')$.

Similarly, by integrating both sides of Eq. (34) with $\overline{g_{B\kappa}}$, we have the exact relation

$$\overline{g_\kappa}(r,r';\omega)=\overline{g_{B\kappa}}(r,r';\omega)+\int dr_2\overline{g_{0\kappa}}(r,r_2;\omega)\times\begin{pmatrix} 0 & B\partial^2/\partial r^2 \\ B\partial^2/\partial r_2 & 0 \end{pmatrix}\times\overline{v_\kappa}(r_3,r_2;\omega)\overline{g_\kappa}(r_2,r';\omega). \tag{54}$$

This equation can be solved by iteration. However, in this case the leapfrog instability eventually creeps in again. We have thus carried out only one iteration.

Some of the results of the self-energy calculation are shown in Figs. 4, 5, and 6. The figures display $V^{mn}_\kappa(\omega;r,r')$ for $\kappa=-1$, $\omega=1$ fm^{-1} and $(mn)=(11)$, (22), and (12), respectively.

We note that the self-energy is nonzero. This implies a dynamical breaking of chiral symmetry. The structure of the self-energy reflects the nonlocal character of the interaction. However, the self-energy is sharply peaked around $r=r'$, reflecting the dominance of the local contribution.

The self-energy is inserted in the Dirac equation which is solved self-consistently for the ground state ($\kappa=-1$). The result is shown in Fig. 7 for the $\kappa(r)$ profile of Fig. 3.

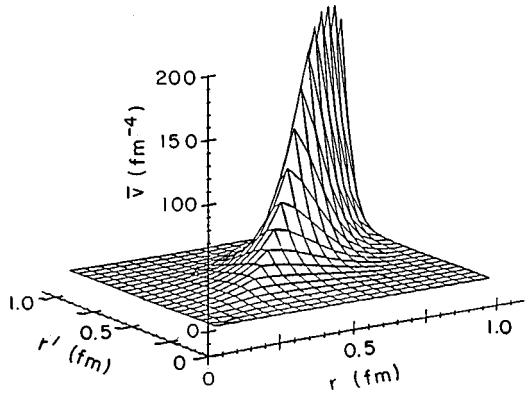

FIG. 5. The quark self-energy on the real ω axis: $\overline{v^{22}_{-1}}(r,r')$.

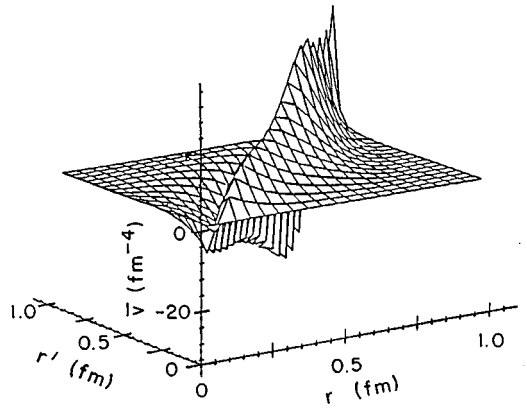

FIG. 6. The quark self-energy on the real ω axis: $\overline{v^{\pm 2}}(r,r')$.

The single-quark energy ϵ is shown in Fig. 8 as a function of κ_v. It does not exhibit a sign of divergence as far as the calculation could be carried out (down to $\kappa_v=0.05$). In fact, ϵ turns out to be quite insensitive to κ_v if κ_v is small. The presented results are thus gratifying.

We have tested our numerical calculation by varying the following numerical parameters: (a) the number $N_{\max}$ of r grid points, (b) the integral limit $r_{\max}$ of r, and (c) the number N_ω of ω grid points. For the actual parameters we have chosen the physical observables all to be insensitive to them.

VII. HADRONIC PROPERTIES

Having calculated the wave function and energy eigenvalue of a single quark in a cavity, we now investigate color-neutral composite systems of N_q valence quarks. Evidently, $N_q=2$ for mesons and $N_q=3$ for baryons. The energy of these systems is calculated in the one-gluon-exchange approximation. Finally, corrections due to the center-of-mass motion and to the σ field are taken into account approximately. Using scaling relations we fix the mass of the nucleon m_N and study the pion mass m_π. Its deviation from zero is a measure of how good our approximations are since

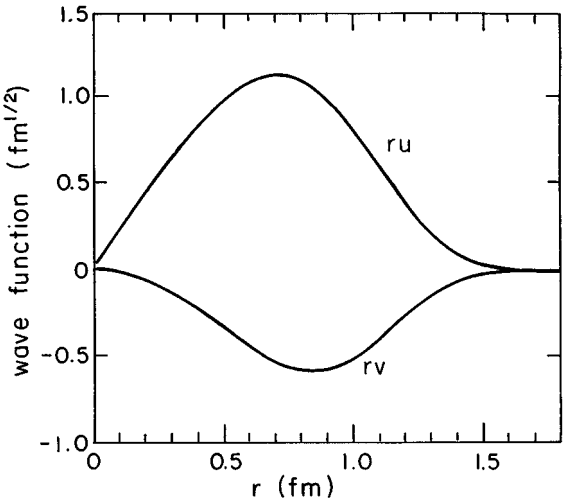

FIG. 7. The quark wave function. $ru(r)$ is the darker line, and $rv(r)$ is the lighter one.

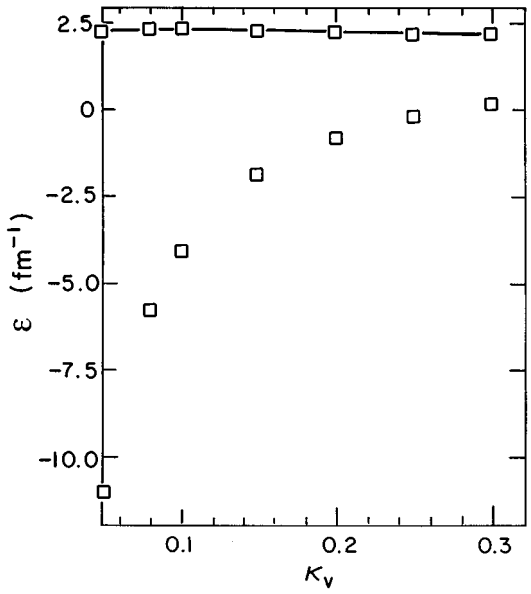

FIG. 8. The single-quark energy ϵ (in fm^{-1}) as a function of κ_v.

the pion should be massless according to Goldstone's theorem.

A. One-gluon-exchange approximation

The one-gluon-exchange interaction energy between quarks (of equal eigenenergy) is given by [2]

$$E_{\rm ex}=\alpha'\int d^3r_1 d^3r_2[j^0(\mathbf{r}_1)D^{00}(\mathbf{r}_1,\mathbf{r}_2)j^0(\mathbf{r}_2) - j(\mathbf{r}_1)\cdot\overleftrightarrow{D}(\mathbf{r}_1,\mathbf{r}_2;0)\cdot\mathbf{j}(\mathbf{r}_2)], \quad (55)$$

with $\alpha'=1/4g_s^2\Sigma_{i<j}\langle\boldsymbol{\lambda}_i\cdot\boldsymbol{\lambda}_j\rangle$. The color matrix element $\langle\boldsymbol{\lambda}_1\cdot\boldsymbol{\lambda}_2\rangle$ has the value $-16/3$ for the pion and $-8/3$ for the nucleon [2]. Taking into account that for both the pion and the nucleon the quarks are in the ground state with $\kappa=-1$, $\mu=\pm 1/2$, the corresponding currents can be evaluated and the exchange energy is ready calculated.

The total energy of quarks and gluons in a hadron with N_q valence quarks is then given by

$$E_{q,g}=N_q\epsilon+E_{\rm ex}. \quad (56)$$

B. Corrections and sigma contributions

Up to now the σ field has been neglected. However, it contributes to the total energy of the bag. The σ field can be reconstructed from $\kappa(r)$ and $\kappa(\sigma)$ given in Eqs. (47) and (3), respectively. Then the σ-field energy is given by

$$E_\sigma=\int[\tfrac{1}{2}(\nabla\sigma)^2+U(\sigma)]d^3r, \quad (57)$$

with the potential $U(\sigma)$ given in Eq. (4). The total energy of the bag is then $E_{\rm bag}=E_{q,g}+E_\sigma$.

We now address the hadronic center-of-mass energy. Since localization of the bag breaks Lorentz invariance, the bag acquires a nonzero total momentum that contributes to the total energy of the system. The easiest way to correct this

effect is to use the following approximate formula (projection [13] would be better but more cumbersome):

$$m_h^2 = E_{\rm bag}^2 - \langle P^2 \rangle_{\rm bag}, \tag{58}$$

with

$$\langle P^2 \rangle_{\rm bag} = N_q \langle P^2 \rangle_q + \langle P^2 \rangle_\sigma . \tag{59}$$

The momentum squared of one quark is given by

$$\langle P^2 \rangle_q = \int d^3r |\nabla q|^2 . \tag{60}$$

In order to calculate $\langle P^2 \rangle_\sigma$, the coherent state approximation [2] is used:

$$\langle P^2 \rangle_\sigma = \int d^3k k^2 \omega_k f_k^2 . \tag{61}$$

f_k are the Fourier transforms of $\sigma(r)$, and ω_k is the σ-field energy in the mode k.

For slowly varying ω_k we finally get

$$\langle P^2 \rangle_\sigma = (m_{\rm GB}^2 + \langle k^2 \rangle)^{1/2} \int d^3r (\nabla \sigma)^2 , \tag{62}$$

with the glueball mass $m_{\rm GB}$.

C. Scaling and the nucleon mass

Scaling can be used to generate new solutions [14] from those presented so far. The equations are invariant under scale transformations where all lengths r are replaced by

$$r \to r' = \lambda r, \tag{63}$$

and all energies and frequencies (including the cutoff $\Lambda_{\rm CDM}$) are replaced by

$$E \to E' = E/\lambda \tag{64}$$

and

$$a \to a' = a/\lambda^2, \quad b' \to b/\lambda . \tag{65}$$

c and α_s are invariant. The σ-field and the gluon field potentials scale as length^{-1}.

D. Numerical results

Throughout our calculations, we use a cutoff $\Lambda_{\rm CDM} = \omega_m = 5$ fm^{-1}. With $l_m = R\omega_m$, the quark wave functions and energies depend on the two parameters R and A from the $\kappa(r)$ profile. The hadron masses additionally depend on the parameters a,b,c of the σ-field potential $U(\sigma)$. In order to minimize the number of free parameters, we assume that $U(\sigma)$ is universal in all hadrons. However, each hadron has a different $\kappa(r)$ profile, reflecting the fact that the hadronic size is not universal.

The numerical procedure is as follows: We choose a potential $U(\sigma)$ and calculate the corrected nucleon mass according to Eq. (58). Using scaling relations we renormalize all dimensional properties by fixing the nucleon mass to its empirical value $m_N = 938$ MeV. With these renormalized properties we now calculate the pion mass as a function of R and A.

TABLE I. Pion masses for $a = 39.9$, $b = -746.2$, $c = 4569.6$, $B = 0.038\ 92$, and $m_{\rm GB} = 1310.8$.

R (fm)	A (fm)	E_q (MeV)	$E_{q,g}$ (MeV)	$\sqrt{\langle P^2 \rangle_Q}$ (MeV)	$\sqrt{\langle P^2 \rangle_\sigma}$ (MeV)	m_π (MeV)
0.6	0.150	404.92	610.61	477.20	189.6	171.31
0.6	0.175	405.81	612.17	476.50	178.3	235.94
0.6	0.200	405.97	613.19	476.10	170.1	290.23
0.6	0.225	405.71	615.40	475.90	164.0	344.06
0.6	0.250	405.22	614.81	475.80	159.4	390.66
0.8	0.150	295.37	452.89	489.10	249.4	344.64
0.8	0.175	296.77	454.19	486.50	232.1	284.70
0.8	0.200	297.20	454.17	484.80	219.0	208.37
0.8	0.225	297.01	453.40	483.70	208.8	61.61
0.8	0.250	296.39	452.22	482.90	200.7	198.74
1.0	0.150	230.69	358.91	485.20	311.7	338.67
1.0	0.175	232.25	360.33	480.00	288.5	238.99
1.0	0.200	232.76	360.09	476.20	270.6	27.71
1.0	0.225	232.60	358.83	473.80	256.3	237.19
1.0	0.250	231.99	356.95	471.70	244.8	342.74
1.2	0.150	194.97	308.29	400.90	375.5	371.10
1.2	0.175	196.45	309.63	398.10	346.6	462.86
1.2	0.200	197.08	309.56	396.10	323.9	540.69
1.2	0.225	197.18	308.61	394.60	305.7	612.00

To this point, the σ field is not self-consistent. We now vary the parameters of the $\kappa(r)$ profile in order to find an extremum in the energy. This is a first approximation to a fully self-consistent treatment. However, we expect the results to be reasonable since the proper shape of the σ field is similar to a Fermi function.

We find that there is always an extremum in A for a given $m_\pi(R)$. This extremum is, however, not necessarily a minimum. Furthermore, the resulting pion mass is small, but nonzero (see Table I). We expect this to be due to the crude method used to correct the effects of the center-of-mass motion. Using projection techniques, Lübeck *et al.* [13] demonstrated how Lorentz invariance is recovered. It turned out that in this framework a significantly lower pion mass is obtained. We therefore assume that this is the (main) source of the finite pion mass.

VIII. SUMMARY AND PROSPECTIVES

Within the framework of the chirally invariant chromodielectric soliton model, the Abelian gluon propagator is solved in configuration space for a color-dielectric function with two parameters. The quark self-energy was obtained by solving the (nonlocal) Schwinger-Dyson equation in configuration space as a function of imaginary energy. Quark wave functions and real eigenvalues were obtained. Bag states were constructed for the pion and the nucleon including one-gluon-exchange mutual interactions between quark pairs. The parameters of the parametrized σ field [or, equivalently, the dielectric function $\kappa(r)$] were varied to extremize the bag energy. Approximate center-of-mass corrections are calculated. Employing scaling relations, the nucleon mass was set to its empirical value. The resulting pion mass was

determined to be small (the actual value depending on the model parameters) but not zero, as demanded by Goldstone's theorem.

Extensions of the present work include the following.

(a) Center-of-mass corrections based on variation after projection. This technique has been studied extensively by Lübeck *et al.* [13] for the Friedberg-Lee soliton and was found to give a significantly lower pion mass. It is certainly more reliable than the prescription $m^2 \approx \langle H \rangle^2 - \langle p^2 \rangle$ used in the present paper.

(b) A ''more'' self-consistent treatment of the soliton field by either solving the differential equation for the σ field or by including more parameters in the functional form of $\kappa(\sigma)$ and $\kappa(r)$.

(c) Calculation of the mutual gluon exchange between quark pairs by full summation of ladder diagrams.

(d) A systematic adjustment of model parameters to fit the properties of all low-lying hadrons. This is not as tedious a task as it might first appear. The parameters of the model are a, b, c, and α_s. The functional form of $\kappa(\sigma)$ also introduces a model dependence, but the results appear to be quite insensitive to that. Of the four, one is set by the nucleon mass using scaling from any given set. Results appear to be relatively insensitive to the ''family'' characterized by b^2/ac [2] but this is related to the glueball mass which is assumed to lie in the range of 1–2 GeV. The key parameters include the nucleon size, magnetic moments, g_A/g_V, and the N-Δ mass splitting. Other hadronic spectra properties are then regarded as predictions of the model.

ACKNOWLEDGMENTS

We are grateful to W. Köpf, G. Krein, and A. Williams for extensive discussions during all phases of this work. S.H. wishes to thank the German Academic Exchange Service (DAAD) and the Cusanuswerk for financial support. This work was supported in part by the U.S. Department of Energy.

APPENDIX

In this appendix the self-energy coefficients $\mathcal{A}$, $\mathcal{B}$, and $\mathcal{C}$ from Sec. IV B [Eqs. (37)–(39)] are explicitly evaluated.

We start with formula (5.9.15) of Edmonds [15]:

$$\sigma_q \chi_\nu = \sqrt{3} \langle 1/2, \nu, 1, q | 1/2, q+\nu \rangle \chi_{q+\nu}. \tag{A1}$$

Note that we use throughout our calculations the phase convention of Edmonds. With the definitions

$$\mathcal{Y}_{\kappa\mu}(\Omega) \equiv \mathcal{Y}^{\,l_\kappa}_{\,j_\kappa \mu}(\Omega) \equiv \sum_{\nu m} \langle l_\kappa, m, 1/2, \nu | j_\kappa, \mu \rangle Y_{l_\kappa m} \chi_\nu, \tag{A2}$$

$$\boldsymbol{\mathcal{Y}}_{ll'm}(\Omega) \equiv \sum_{q m'} \langle l', m', 1, q | l, m \rangle Y_{l'm'} \boldsymbol{\epsilon}_q, \tag{A3}$$

$$\boldsymbol{\epsilon}_{\pm 1} = \mp \frac{\hat{\mathbf{x}} \pm i \hat{\mathbf{y}}}{\sqrt{2}}, \quad \boldsymbol{\epsilon}_0 = \hat{\mathbf{z}}, \tag{A4}$$

we get

$$\begin{aligned}
\boldsymbol{\mathcal{Y}}_{ll'm}(\Omega) \cdot \boldsymbol{\sigma} \mathcal{Y}_{\kappa\mu}(\Omega) &= \sum_{m_1 q m_2 \nu} \langle l', m_1, 1, q | l, m \rangle Y_{l'm_1} \sigma_q \langle l_\kappa, m_2, 1/2, \nu | j_\kappa, \mu \rangle \chi_\nu Y_{l_\kappa m_2} \\
&= \sum_{m_1 q m_2 \nu L M \nu'} \langle l', m_1, 1, q | l, m \rangle Y_{LM} \langle l_\kappa, m_2, 1/2, \nu | j_\kappa, \mu \rangle \langle l', 0, l_\kappa, 0 | L, 0 \rangle \\
&\quad \times \langle l', m_1, l_\kappa, m_2 | L, M \rangle \sqrt{\frac{(2l'+1)(2l_\kappa+1)}{4\pi(2L+1)}} \sqrt{3} \langle 1/2, \nu, 1, q | 1/2, \nu' \rangle \chi_{\nu'} \\
&= \sum_{\mu' j L} (-1) \sqrt{(2l+1)(2j_\kappa+1)(2l_\kappa+1)(2l'+1) 3/2\pi} \langle (l, m, j_\kappa, \mu | j, \mu' \rangle \langle l', 0, l_\kappa, 0 | L, 0 \rangle \\
&\quad \times \begin{Bmatrix} L & 1/2 & j \\ l' & 1 & l \\ l_\kappa & 1/2 & j_\kappa \end{Bmatrix} \mathcal{Y}^{\,L}_{\,j\mu'}.
\end{aligned} \tag{A5}$$

Here we have used the contraction formula for spherical harmonics [Edmonds, Eq. (5.16)] and the definition of the $9j$ symbols [Edmonds, Eq. (6.4.3)].

Similarly,

$$2\hat{\mathbf{r}}\cdot\boldsymbol{\mathcal{Y}}_{ll'm}(\Omega)\mathcal{Y}_{\kappa\mu}(\Omega)=\sum_{m_1qm_2\nu}2\langle l',m_1,1,q|l,m\rangle Y_{l'm_1}\sqrt{4\pi 3}\;Y_{1q}\langle l_\kappa,m_2,1/2,\nu|j_\kappa,\mu\rangle\chi_\nu Y_{l_\kappa m_2}$$
$$=\sum_{m_1qm_2\nu}2\langle l',0,1,0|l,0\rangle Y_{lm}\sqrt{\frac{4\pi}{3}\frac{(2+1)(2l'+1)}{4\pi(2l+1)}}\,\langle l_\kappa,m_2,1/2,\nu|j_\kappa,\mu\rangle\chi_\nu Y_{l_\kappa m_2}$$
$$=\sum_{jL\mu'}(-1)^{1/2+l+l_\kappa+j}\sqrt{\frac{(2l_\kappa+1)(2j_\kappa+1)(2l'+1)}{\pi}}\,\langle l',0,1,0|l,0\rangle\langle l,0,l_\kappa,0|L,0\rangle$$
$$\times\begin{Bmatrix}j_\kappa & 1/2 & l_\kappa\\ L & l & j\end{Bmatrix}\langle l,m,j_\kappa,\mu|j,\mu'\rangle\mathcal{Y}^{\,L}_{j\mu'} \tag{A6}$$

and

$$Y_{lm}(\Omega)Y_{\kappa\mu}(\Omega)=\sum_{m_1qm_2\nu}Y_{lm}\langle l_\kappa,m_2,1/2,\nu|j_\kappa,\mu\rangle\chi_\nu Y_{l_\kappa m_2}$$
$$=\sum_{jL\mu'}(-1)^{1/2-j_\kappa+l_\kappa+2j}\sqrt{\frac{(2l_\kappa+1)(2j_\kappa+1)(2l+1)}{4\pi}}\,\langle l,0,l_\kappa,0|L,0\rangle$$
$$\times\begin{Bmatrix}j_\kappa & 1/2 & l_\kappa\\ L & l & j\end{Bmatrix}\langle j_\kappa,\mu,l,m|j,\mu'\rangle\mathcal{Y}^{\,L}_{j\mu'}. \tag{A7}$$

According to Eq. (A5), the expression $\Sigma_{m\mu}\boldsymbol{\mathcal{Y}}_{ll'm}(\Omega)\cdot\boldsymbol{\sigma}\mathcal{Y}_{\kappa\mu}(\Omega)\mathcal{Y}^\dagger_{\kappa\mu}(\Omega')\boldsymbol{\sigma}\cdot\boldsymbol{\mathcal{Y}}^*_{ll''m}(\Omega')$ is proportional to $\delta_{jj'}$ and $\delta_{\mu\mu'}$. Now L and L' have to be equal or differ by 1. However, $\langle l',0,l_\kappa,0|L,0\rangle\langle l'',0,l_\kappa,0|L',0\rangle$ vanishes if $|L-L'|$ is odd, since $l'-l''$ is even, and so only terms with $L=L'$ (or $\kappa'=\kappa''$) contribute. Thus

$$\sum_{m\mu}\boldsymbol{\mathcal{Y}}_{ll'm}(\Omega)\cdot\boldsymbol{\sigma}\mathcal{Y}_{\kappa\mu}(\Omega)\mathcal{Y}^\dagger_{\kappa\mu}(\Omega')\boldsymbol{\sigma}\cdot\boldsymbol{\mathcal{Y}}^*_{ll''m}(\Omega')=\sum_{\kappa\mu'}\mathcal{A}^{\kappa'\kappa}_{ll'l''}\mathcal{Y}_{\kappa'\mu'}(\Omega)\mathcal{Y}^\dagger_{\kappa'\mu'}(\Omega'). \tag{A8}$$

The symmetry relation $\mathcal{A}^{\kappa'\kappa}_{ll'l''}=\mathcal{A}^{\kappa'\kappa}_{ll''l'}$ holds.

Similarly, according to Eq. (A2), the expression $\Sigma_{m\mu}2\hat{\mathbf{r}}\cdot\boldsymbol{\mathcal{Y}}_{ll'm}(\Omega)\mathcal{Y}_{\kappa\mu}(\Omega)\mathcal{Y}^\dagger_{\kappa\mu}(\Omega')\boldsymbol{\sigma}\cdot\boldsymbol{\mathcal{Y}}_{ll'm}(\Omega')$ is proportional to $\delta_{jj'}$ and $\delta_{\mu\mu'}$. Now L and L' have again to be equal or differ by 1. However, $\langle l,0,l_\kappa,0|L,0\rangle\langle l',0,1,0|l,0\rangle\langle l'',0,l_\kappa,0|L',0\rangle\rangle$ vanishes if $|L-L'|$ is even, since $l'-l''$ is even, and so only terms with $L=L'\pm1$ (or $\kappa'=-\kappa''$) contribute. Thus

$$\sum_{m\mu}2\hat{\mathbf{r}}\cdot\boldsymbol{\mathcal{Y}}_{ll''m}(\Omega)\mathcal{Y}_{\kappa\mu}(\Omega)\mathcal{Y}^\dagger_{\kappa\mu}(\Omega')\boldsymbol{\sigma}\cdot\boldsymbol{\mathcal{Y}}^*_{ll''m}(\Omega')=\sum_{\kappa\mu'}\widetilde{\mathcal{B}}^{\kappa'\kappa}_{ll'l''}\mathcal{Y}_{\overline{\kappa'}\mu'}(\Omega)\mathcal{Y}^\dagger_{\kappa'\mu'}(\Omega'). \tag{A9}$$

Similarly, we have

$$\sum_{m\mu}Y_{lm}\mathcal{Y}_{\kappa\mu}(\Omega)\mathcal{Y}^\dagger_{\kappa\mu}(\Omega')Y^*_{lm}(\Omega')=\sum_{\kappa\mu'}\mathcal{C}^{\kappa'\kappa}_{l}\mathcal{Y}_{\kappa'\mu'}(\Omega)\mathcal{Y}^\dagger_{\kappa'\mu'}(\Omega'). \tag{A10}$$

Finally, the quark-gluon coupling coefficients $\mathcal{A}$, $\mathcal{B}$, and $\mathcal{C}$ are given by

$$\mathcal{A}^{\kappa'\kappa}_{ll'l''}=\frac{3}{2\pi}\sqrt{(2l'+1)(2l''+1)}(2j_\kappa+1)(2l_\kappa+1)(2l+1)\langle l',0,l_\kappa,0|l_{\kappa'},0\rangle\langle l'',0,l_\kappa,0|l_{\kappa'},0\rangle$$
$$\times\begin{Bmatrix}l_{\kappa'} & 1/2 & j_{\kappa'}\\ l' & 1 & l\\ l_\kappa & 1/2 & j_\kappa\end{Bmatrix}\begin{Bmatrix}l_{\kappa'} & 1/2 & j_{\kappa'}\\ l'' & 1 & l\\ l_\kappa & 1/2 & j_\kappa\end{Bmatrix}, \tag{A11}$$

$$\widetilde{\mathcal{B}}^{\kappa'\kappa}_{ll'l''}=(-1)^{-1/2+l+l_\kappa+j_{\kappa'}}\sqrt{3/2(2l'+1)(2l''+1)(2l+1)}\,\frac{(2l_\kappa+1)(2j_\kappa+1)}{\pi}\langle l'',0,l_\kappa,0|l_{\kappa'},0\rangle\langle l',0,1,0|l,0\rangle$$

$$\times\begin{Bmatrix} j_\kappa & 1/2 & l_\kappa \\ l_{\overline{\kappa'}} & l & j_{\kappa'}\end{Bmatrix}\begin{Bmatrix} l_{\kappa'} & 1/2 & j_{\kappa'} \\ l'' & 1 & l \\ l_\kappa & 1/2 & j_\kappa\end{Bmatrix}, \tag{A12}$$

$$\mathcal{C}^{\kappa'\kappa}_l=\frac{(2l_\kappa+1)(2j_\kappa+1)(2l+1)}{4\pi}\langle l,0,l_\kappa,0|l_{\kappa'},0\rangle^2\begin{Bmatrix} j_\kappa & 1/2 & l_\kappa \\ l_{\kappa'} & l & j_{\kappa'}\end{Bmatrix}^2. \tag{A13}$$

Furthermore,

$$\sum_{m\mu}\boldsymbol{\mathcal{Y}}_{ll'm}(\Omega)\cdot\boldsymbol{\sigma}\sigma_r\mathcal{Y}_{\kappa\mu}(\Omega)\mathcal{Y}^\dagger_{\kappa\mu}(\Omega')\boldsymbol{\sigma}\cdot\boldsymbol{\mathcal{Y}}^*_{ll''m}(\Omega')=\sum_{m\mu}[2\hat{\mathbf{r}}\cdot\boldsymbol{\mathcal{Y}}_{ll''m}(\Omega)-\sigma_r\boldsymbol{\mathcal{Y}}_{ll'm}(\Omega)\cdot\boldsymbol{\sigma}]\mathcal{Y}_{\kappa\mu}(\Omega)\mathcal{Y}^\dagger_{\kappa\mu}(\Omega')\boldsymbol{\sigma}\cdot\boldsymbol{\mathcal{Y}}^*_{ll''m}(\Omega')$$

$$=\sum_{\kappa\mu'}\mathcal{B}^{\kappa'\kappa}_{ll'l''}\sigma_r\mathcal{Y}_{\kappa'\mu'}(\Omega)\mathcal{Y}^\dagger_{\kappa'\mu'}(\Omega'). \tag{A14}$$

In that very last step we have used Eqs. (A5) and (A6) as well as the identity $\sigma_r\,\mathcal{Y}_{\kappa\mu}=-\mathcal{Y}_{\overline{\kappa\mu}}$ and the identification

$$\mathcal{B}^{\kappa'\kappa}_{ll'l''}\equiv-\mathcal{A}^{\kappa'\kappa}_{ll'l''}-\widetilde{\mathcal{B}}^{\kappa'\kappa}_{ll'l''}. \tag{A15}$$

Working out the Hermitian conjugate of Eqs. (A8) and (A9) we get the symmetry relations $\mathcal{A}^{\kappa'\kappa}_{ll'l''}=\mathcal{A}^{\kappa'\kappa}_{ll''l'}$ and $\mathcal{B}^{\kappa'\kappa}_{ll'l''}=\mathcal{B}^{-\kappa'-\kappa}_{ll''l'}$.

[1] G. Fai, R. J. Perry, and L. Wilets, Phys. Lett. B **208**, 1 (1988).
[2] L. Wilets, *Nontopological Solitons* (World Scientific, Singapore, 1989).
[3] R. Friedberg and T. D. Lee, Phys. Rev. D **15**, 1694 (1977); **16**, 1096 (1977); **18**, 2613 (1978).
[4] G. Krein, P. Tang, L. Wilets, and A. G. Williams, Phys. Lett. B **212**, 362 (1988); Nucl. Phys. **A523**, 548 (1991).
[5] Y. Nambu and G. Jona-Lasinio, Phys. Rev. **122**, 345 (1961); **124**, 246 (1961).
[6] V. Bernard, R. Brockmann, M. Schaden, W. Weise, and E. Werner, Nucl. Phys. **A412**, 349 (1984).
[7] M. Bickeböller, R. Goldflam, and L. Wilets, J. Math. Phys. (N.Y.) **26**, 1810 (1985).
[8] P. Tang and L Wilets, J. Math. Phys. (N.Y.) **31**, 1661 (1991).
[9] E. H. Wichmann and N. M. Kroll, Phys. Rev. **101**, 843 (1956).
[10] M. Gyulassy, Nucl. Phys. **A244**, 497 (1975).
[11] U. Ritschel, L. Wilets, J. J. Rehr, and M. Grabiak, J. Phys. G **18**, 1889 (1992).
[12] G. Dahlquist, Å. Björk, and N. Anderson, *Numerical Methods* (Prentice-Hall, Englewood Cliffs, NJ, 1974).
[13] E. G. Lübeck, M. C. Birse, E. M. Henley, and L. Wilets, Phys. Rev. D **33**, 234 (1986); E. G. Lübeck, E. M. Henley, and L. Wilets, *ibid.* **35**, 2809 (1987).
[14] R. Goldflam and L. Wilets, Phys. Rev. D **25**, 1951 (1982).
[15] A. Edmonds, *Angular Momentum in Quantum Mechanics* (Princeton University Press, Princeton, NJ, 1957).